PCCP

PAPER

View Article Online
View Journal | View Issue

Cite this: *Phys. Chem. Chem. Phys.*, 2018, **20**, 7217

Viable aromatic Be_nH_n stars enclosing a planar hypercoordinate boron or late transition metal†

Xue-Feng Zhao,‡[a] Jia-Jia Li,‡[a] Hai-Ru Li,[a] Caixia Yuan,[a] Xinxin Tian,[a] Si-Dian Li,[a] Yan-Bo Wu,*[a] Jin-Chang Guo*[ab] and Zhi-Xiang Wang*[c]

Received 11th October 2017,
Accepted 15th February 2018

DOI: 10.1039/c7cp06955c

rsc.li/pccp

Monocyclic B_n rings can act as *n*-electron σ-donors to stabilize a non-classical planar hypercoordinate atom at ring center, forming wheel-like structures. Herein, we report that Be_nH_n rings can also serve as *n*-electron σ-donors to construct star-like structures including B©$Be_6H_6^+$ and TM©$Be_7H_7^q$ (TM is a group 10–12 metal with q = −1, 0, and 1, respectively) by complying with octet or 18-electron rules. Electronic structure analyses show that these species are stabilized by the σ-donation and π-backdonation between the central atom and the peripheral Be_nH_n ring, the favorable Coulomb attraction due to the negative–positive–negative charge population pattern on the central atom, the middle Be_n layer, and the outer H_n layer, as well as the σ–π double aromaticity. Importantly, three of the ten species, including B©$Be_6H_6^+$, Cu©Be_7H_7, and Au©Be_7H_7, were confirmed to be kinetically stable global minima, thereby providing promising targets for experimental preparations.

Introduction

Boron prefers forming multicenter bonding due to its electron deficiency, as represented by the well-known polyhedral boranes.[1] In the past decades, such bonding preference has been further utilized to stabilize/construct novel planar structures with non-classical chemical bonding. Examples include those with planar hypercoordinate carbon (phC),[2] planar/quasi-planar boron clusters B_n (n = 7–19),[3] X-centered boron wheels X©B_n (n = 6–10, X = group 2, 13, and 14 atoms or transition metals),[4] and multiple X-centered boron rings X_m©B_n (n = 7–12, X = Be and C, m = 2–6).[5] In these structures, the boron atoms in B_n rings commonly use two valence electrons to form bonds with their neighbors in the ring and one valence electron to form centripetal bonding with central atom(s), thus B_n rings act as *n*-electron σ-donors.

Beryllium also exhibits electron deficiency. For examples, Yáñez *et al.* proposed that the electron deficient beryllium atom in BeX_2 (X = H, F, Cl, and OH) is Lewis acidic (having σ-hole), thus can accept lone pair electrons from a variety of Lewis bases.[6] Recently, such a σ donor–acceptor interaction in beryllium-containing structures have been investigated and further extended to interactions between electron-rich molecules and the π-hole established in some beryllium compounds.[7] However, compared to the rich boron-based structures, beryllium-based structures are rather limited. This is probably due to the high toxicity of beryllium and its compounds, which discourages conventional experimental study.[8] As such, reliable theoretical computation is an ideal approach to explore beryllium-based structures[9] by providing promising targets for effective experimental exploration.

Similar to boron, beryllium has been used to stabilize phC[10] but not to form structures similar to X©B_n or X_m©B_n because beryllium is one electron less than boron, thus a bare beryllium ring would have no electrons to form centripetal bonding with central atom(s). Nevertheless, on the basis of our previous studies,[9,10b,j,n,p] we envisioned that Be_nH_n rings may overcome the problem, because a Be_nH_n ring may use n three-center two-electron (3c-2e) bonds to construct a ring equivalent to B_n ring, thus having n electrons left for forming centripetal bonding with central atom. In the following, we demonstrate that Be_nH_n indeed can serve as *n*-electron σ-donors, forming planar or quasi-planar structures X©Be_nH_n. Related to the present work, we note some experimental studies on BeH_2 oligomers and lithium beryllium hydrides.[11]

Computational methods

The structures shown in Fig. 1 were optimized and characterized to be true minima by frequency analysis calculations at the

[a] *The Key Lab of Materials for Energy Conversion and Storage of Shanxi Province, Institute of Molecular Science, Shanxi University, Taiyuan, Shanxi 030006, People's Republic of China. E-mail: wyb@sxu.edu.cn*
[b] *Institute of Materials Science and Department of Chemistry, Xinzhou Teacher's University, Xinzhou, Shanxi 034000, People's Republic of China. E-mail: gjchang01@yahoo.com*
[c] *College of Chemistry and Chemical Engineering, University of Chinese Academy of Sciences, Beijing 100049, People's Republic of China. E-mail: zxwang@ucas.ac.cn*

† Electronic supplementary information (ESI) available: The figures describing the AdNDP and NICS results of **3–10**, the geometries and relative energies of lowest five isomers of **1–10**, the necessary Cartesian coordinates of the structures mentioned in this work. See DOI: 10.1039/c7cp06955c

‡ Xue-Feng Zhao and Jia-Jia Li contributed equally to this work.

B3LYP/BSI level, where BSI denotes a mixed basis set, cc-pVTZ for elements lighter than Ni and cc-pVTZ-PP for TMs heavier than Cu. The B3LYP/BSI results were calibrated using double hybrid functional at the B2PLYP-D/BSI level. The natural bond orbital (NBO)[12] analyses and the nucleus-independent chemical shift (NICS)[13] calculations were performed at the B3LYP/BSI. In order to further understand the chemical bonding pattern of these structures, adaptive natural density partitioning (AdNDP)[14] analyses were carried out at the B3LYP level with 6-31G basis set for elements lighter than Zn and LANL2DZ for other TMs. AdNDP is an extension of NBO analysis and describes the electronic structure of a molecular system in terms of *n*-center two-electron bonds (*n* ranges from 1 to the total number of atoms in a molecule). Thus, AdNDP analysis recovers not only the Lewis elements such as lone pairs and 2c-2e bond, but also the delocalized *n*c-2e bonds. The searches for global minima were carried out by exploring potential energy surfaces, using both the stochastic search[15] and particle swarming optimization (PSO)[16] algorithms. The initially generated structures were optimized at the B3LYP/6-31G(d) level for $Be_6H_6B^+$ composition and B3LYP/LANL2DZ level for $Be_7H_7TM^q$ composition. Then, the twenty lowest energy minima were re-optimized at the B3LYP/BSI level. Finally, the energies of the lowest ten isomers selected from re-optimizations were improved at the CCSD(T)/BSI level and corrected with the B3LYP/BSI zero-point energies. Born–Oppenheimer molecular dynamic (BOMD)[17] simulations were conducted at the B3LYP/BSII level for 50 picoseconds, where BSII denotes a basis set with 6-31G(d) for Be, B, and H and SDD for Cu, Pd, and Au. The stochastic search were realized using GXYZ program,[18] the PSO studies were performed using CALYPSO program,[19] the CCSD(T) calculations were carried out using the MolPro 2012.1 package,[20] and all other calculations were performed using the Gaussian 09 package.[21]

Results and discussion

X-centered (Ⓒ) Be_5H_5 and Be_6H_6 stars

Similar to B_n rings, Be_nH_n rings alone are not energy minima, requiring a central atom to support a ring structure. In order to achieve optimal geometric and electronic structure, we envisioned that Be_nH_n ring should match the center atom in size and the central atom had better meet the octet or 18-electron (18e) rule. Apparently, Be_4H_4 is too small to accommodate any of group 14 atom or group 15 cation. The octet rule allows Be_5H_5 ring to adopt a group 13 atom or group 14 cation at the center, but even the smallest B and C^+ were found to be too large to suit the ring. According to our calculations at the B3LYP/BSI level (see computational details in ESI†), the geometry optimization gave quasi-planar C_{5v} rather than planar D_{5h} structures for BⒸBe_5H_5 and CⒸ$Be_5H_5^+$ (Fig. S1 in ESI†). In spite of the size-mismatch, the two structures feature large HOMO–LUMO gaps (4.41 and 6.09 eV, respectively) and well-maintained Be_5H_5 ring due to meeting the octet rule. Neutral nitrogen atom is smaller than boron but the planar NⒸBe_5H_5 (see Fig. S1, ESI†) is a fifth-order saddle point. Moreover, none of the imaginary frequencies describes a motion that squeezes the N atom out of Be_5H_5 plane. Because of the very small HOMO–LUMO gap (1.14 eV) of the species, we attribute the non-minimum nature of the species to that the species does not meet octet role, although the geometric factor indicates that N is too small to enable effective interaction between the central atom and peripheral ring may contribute. The results of these species indicate that the fulfillment of the octet rule is an important requirement but not the sole one.

Next, we considered Be_6H_6 ring, a six-electron σ-donor. Although the ring is too small to accommodate a group 2 atom (*e.g.* beryllium) to give a planar structure, it nicely fits a smaller B^+. Our calculations show that D_{6h} BⒸ$Be_6H_6^+$ (**1** in Fig. 1) featuring a perfect planar hexacoordinate boron (phB) is an

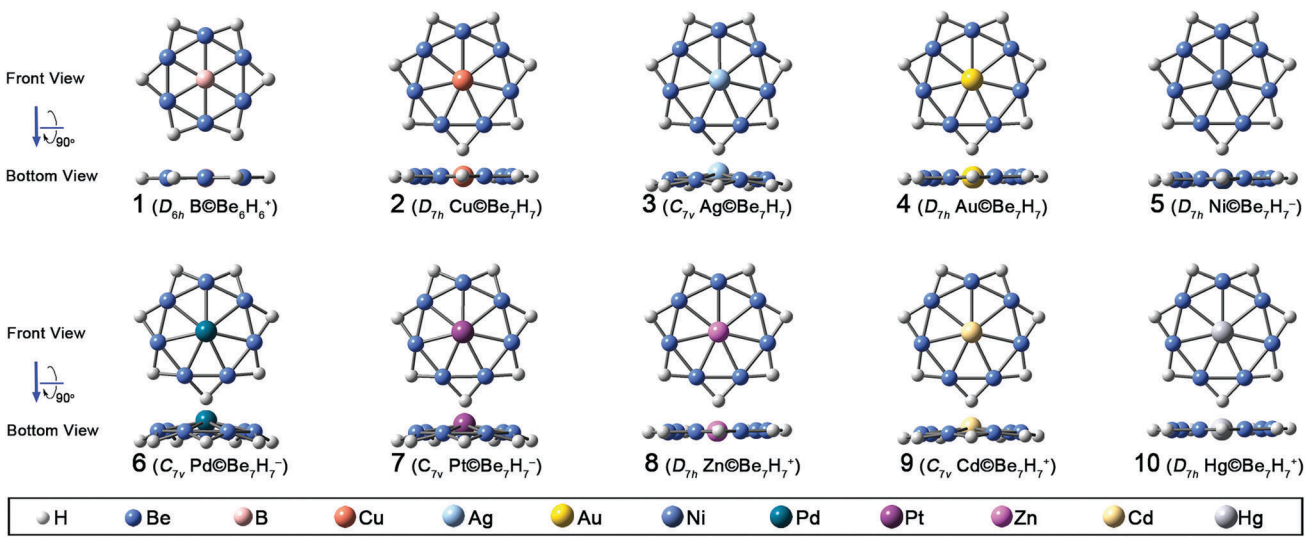

Fig. 1 B3LYP/BSI-optimized structures of **1–10**.

Table 1 Key B3LYP/BSI results of **1–10**, including the lowest vibrational frequencies (ν_{min}, in cm^{-1}), the HOMO–LUMO gaps (gap, in eV), the interatomic distances (R, in Å), the Wiberg bond indices (WBI), and the NBO charges (Q, in $|e|$) of X, Be, and H atoms

			R			Q			WBI		
	ν_{min}	Gap	Be–X	Be–Be	Be–H	X	Be	H	Be–X	Be–Be	Be–H
1	78	4.04	1.887	1.887	1.447	−1.47	+0.59	−0.18	0.64	0.29	0.47
2	82	2.56	2.190	1.901	1.464	−0.96	+0.35	−0.21	0.51	0.41	0.46
3	69	2.60	2.273	1.956	1.473	−0.77	+0.34	−0.23	0.50	0.42	0.46
4	49	2.93	2.253	1.955	1.477	−0.96	+0.36	−0.22	0.57	0.39	0.46
5	44	2.68	2.167	1.877	1.485	−1.17	+0.24	−0.21	0.53	0.46	0.47
6	94	2.63	2.255	1.913	1.480	−0.96	+0.22	−0.22	0.51	0.47	0.46
7	93	2.90	2.239	1.916	1.487	−1.12	+0.24	−0.22	0.59	0.49	0.46
8	80	2.60	2.248	1.950	1.446	−0.78	+0.47	−0.21	0.53	0.36	0.46
9	41	2.62	2.330	2.009	1.458	−0.55	+0.46	−0.23	0.53	0.37	0.45
10	70	2.92	2.307	2.002	1.459	−0.74	+0.48	−0.23	0.57	0.34	0.46

energy minimum with the smallest vibrational frequency (ν_{min}) of 78 and 57 cm^{-1} at the B3LYP/BSI and B2PLYP-D/BSI levels, respectively. The large HOMO–LUMO gap (4.04 eV) of **1** is indicative of its optimal electronic structure. Due to the D_{6h} symmetry, **1** has identical Be–Be and Be–B bond distances of 1.887 Å at B3LYP/BSI level. The Be–H distance in **1** is 1.447 Å (see Table 1). Again, C©Be_6H_6 and N©$Be_6H_6^+$ that do not meet the octet rule have small HOMO–LUMO gaps and imaginary frequencies tending to destroy the Be_6H_6 ring. Previously, we found that C©$Be_5H_5^+$ prefers a non-planar C_{5v} structure, while C©$Be_5F_5^+$ favor a planar D_{5h} structure.[10q] In contrast, though B©$Be_6H_6^+$ has a planar D_{6h} structure, B©$Be_6F_6^+$ adopts the non-planar C_{2v} structure (see Fig. S1, ESI†). We attribute the difference between the two scenarios to the ring expansion due to the replacement of H atoms with F atoms, which makes the oversized carbon in D_{5h} C©$Be_5H_5^+$ fit to the expanded Be_5F_5 ring. As a comparison, boron fits the Be_6H_6 ring, but it is too small to fit the expanded Be_6F_6 ring. The butterfly-shape distortion of Be_6F_6 ring in B©$Be_6F_6^+$ enables the more efficient bonding to carbon, suggesting that the 6-electron σ-donor nature of Be_6F_6 holds true. Note that its large HOMO–LUMO gap of 4.61 eV also indicates its good electronic structure.

To understand the electronic structure of **1**, we performed AdNDP analyses. As shown in Fig. 2, among ten pairs of valence electrons of **1**, six pairs form six Be–H–Be 3c-2e σ bonds with occupation number (ON) of 1.99 $|e|$ (see **A**). The remaining four pairs form bonding orbitals with central boron atom, including three thirteen-center two electron (13c-2e) σ bonds with ON = 2.00 $|e|$ (see **B–D**) and one seven-center two-electron (7c-2e) π bond with ON = 2.00 $|e|$ (see **E**). The three σ bonds describe the σ-donation of Be_nH_n ring to boron and the π bond describes the π-back-donation of boron to Be_nH_n ring. Because boron is involved in these four bonds (**B–E**), the valence shell of boron have eight electrons, fulfilling the octet rule. Moreover, **1** involves six delocalized σ electrons and two delocalized π electrons, meeting the Huckel rule, thus the species features σ–π double aromaticity. To corroborate this, the NICS values were calculated for the ghost atoms located at the center of Be–B–Be triangle and up to 2 Å above this point as well as above the center B atom. As shown in Fig. 3, the notable negative

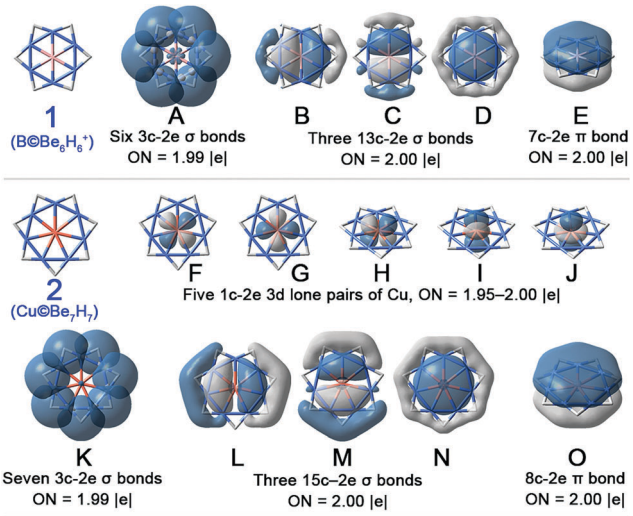

Fig. 2 AdNDP view of chemical bonding in B©$Be_6H_6^+$ (**1**) and Cu©Be_7H_7 (**2**).

NICS value (−16.7 ppm) at the center of Be–B–Be triangle indicates the σ-aromaticity and the large negative NICS values of −13.2 and −23.5 ppm (at the points 1 Å above this point and above the center B atom, respectively) indicate the π aromaticity of the species.

To assess the bonding strength, we also performed NBO analyses on **1**. As shown in Table 1, the Wiberg bond index of Be–B (WBI_{Be-B} = 0.64) indicate the relatively strong Be–B covalent bonding. The Wiberg bond index of Be–H bond (WBI_{Be-H} = 0.47) agrees with the assignment of 3c-2e bond to Be–H–Be triangles. The natural charges on B, Be, and H atoms are −1.47, +0.59, and −0.18 $|e|$, respectively, thus **1** features the charge distribution pattern of negative–positive–negative (abbreviated as "−+−"), which favors the stabilization of the species *via* Coulomb attractions. In addition, the negative charge on boron characterizes the electron donor of Be_6H_6 ring.

TM©Be_7H_7 and TM©Be_8H_8 stars

Next to Be_6H_6 ring, we explored the bonding capacity of Be_7H_7, a seven-electron σ-donor. Our attempts to suit an alkali metal atom or an alkali earth metal cation in Be_7H_7 ring did not give planar structures (Fig. S1, ESI†), which we attributed to the weak covalent bonding capacity of these metals and the geometric mismatch between the ring and the central atoms. Since no other main group atom can meet the octet rule when fitting

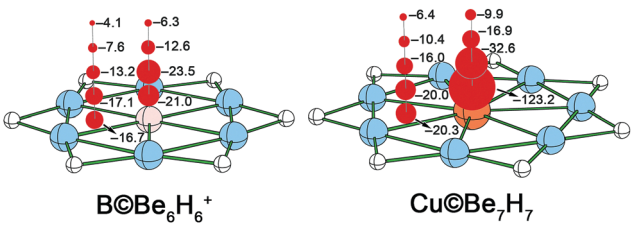

Fig. 3 NICS values of B©$Be_6H_6^+$ (**1**) and Cu©Be_7H_7 (**2**). The H, Be, B, and Cu are shown in white, light blue, pink, and orange, respectively. Along the vertical line, the NICS points (red balls) are 0.5 Å apart from their neighbors.

into Be_7H_7 ring, we considered transition metals by complying with the 18e rule, where such ring may adopt a group 11 metal atom (Cu, Ag, or Au). Indeed, geometric optimization at both B3LYP/BSI and B2PLYP-D/BSI levels show that Cu©Be_7H_7 (**2**) and Au©Be_7H_7 (**4**) have perfect planar D_{7h} structures (Fig. 1) and Ag©Be_7H_7 (**3**) has a quasi-planar C_{7v} structure. In addition, we also examined group 10 and 12 metals, which led to the anionic species TM©$Be_7H_7^-$ (TM = Ni, Pd, and Pt, **5–7** in Fig. 1) and cationic TM©$Be_7H_7^+$ (TM = Zn, Cd, and Hg, **8–10** in Fig. 1) meeting the 18e rule. At both B3LYP/BSI and B2PLYP-D/BSI levels, Ni©$Be_7H_7^-$ (**5**), Zn©$Be_7H_7^+$ (**8**), and Hg©$Be_7H_7^+$ (**10**) have planar D_{7h} structures, while others adopt quasi-planar C_{7v} symmetry. At the B3LYP/BSI level, the Be–TM distances range from 2.167 to 2.330 Å and Be–Be distances lies between 1.877 and 2.009 Å (Table 1). In general, the Be–TM and Be–Be distances in the C_{7v} structures are longer than those in D_{7h} structures, reflecting that the TMs in D_{7h} structures are more suitable for a Be_7H_7 ring.

We also performed AdNDP analyses on **2–10**. The results of **2** are included in Fig. 2 and the similar results for **3–10** are given in Fig. S2 (ESI†). Among the sixteen valence electron pairs of **2**, five pairs can be regarded as the 3d lone pairs of copper with ONs ranging from 1.95 to 2.00 $|e|$ (see **F–J** in Fig. 2), seven pairs form seven Be–H–Be 3c-2e σ bonds with ON = 1.99 $|e|$ (see **K**), three pairs form three fifteen-center two-electron (15c-2e) σ bonds with ON = 2.00 $|e|$ (see **L–N**,) which describe the σ-donation of Be_7H_7 ring to copper, and the remaining one pair forms an eight-center two-electron (8c-2e) π bond with ON = 2.00 $|e|$ (see **O**), which corresponds to the π back-donation from copper to Be_7H_7 ring. Together, the five 3d lone pairs and the four delocalized orbitals fill 18 electrons into the valence shell of copper atom, meeting the 18e rule.

Similar to **1**, **2** also feature σ–π double aromaticity due to the three delocalized σ orbitals and one delocalized π orbital, as evidenced by the NICS values (Fig. 3). The center of Be–Cu–Be triangle has a negative NICS value of −20.3 ppm, suggesting the σ aromaticity, and the large negative NICS values of −16.0 and −32.6 ppm at points 1.0 Å above the molecular plane suggest the π aromaticity. The NICS results of **3–10** are similar to that of **2** and are given in Fig. S3 (ESI†).

The NBO results of **2–10** are similar to that of **1**. First, these species also feature "− + −" charge population pattern with TM atoms, beryllium atoms, and hydrogen atoms bearing negative, positive, and negative charges, respectively. The negative charges on TM atoms (−0.55 to −1.17 $|e|$) in **2–10** reveals the electron donation nature of Be_7H_7 ring. Second, the WBI values for Be–H bonding range from 0.45 to 0.47, suggesting the formation of Be–H–Be 3c-2e bonds and those for Be–TM bonding ranging from 0.50 to 0.57 indicate the formation of multicenter covalent bonds between Be_n and TM center.

Further enlarging the Be_nH_n ring, we considered Be_8H_8. The 18e rule requires the ring to adopt a group 9–11 TM atom, giving anionic, neutral, and cationic TM©$Be_8H_8^q$ (q = −1, 0, and +1), respectively. However, our calculations showed that none of them adopts D_{8h} structure, because a Be_8H_8 ring is too large to effectively interact with a central TM atom, as implied by the optimized butterfly-like structures that allow the more effective Be–TM bonding (Fig. S4, ESI†).

Stability consideration

Although **1–10** are energy minima with optimal electron structure, to be accessible experimentally, they should be stable both thermodynamically and kinetically. The thermodynamic stabilities of **1–10** are studied by extensive explorations on their potential energy surfaces using both stochastic search and PSO algorithms. According to our results, **1**, **4**, and **6** are global energy minima, which are 19.8, 17.9, and 1.4 kcal mol^{-1} lower than their second lowest isomers, respectively; **2** is the second lowest energy isomer and the global minimum can be seen as a Be©Be_6H_6 structure with an out-of-plane bonded Cu–H moiety (see **2a** in Fig. S5 of ESI†). However, **2** is only 0.7 kcal mol^{-1} higher than **2a**, thus it should be competitive in the experiments. In contrast, **3**, **5**, and **7–10** are local minima, which are 8.0, 20.4, 4.4, 3.6, 21.5, and 12.7 kcal mol^{-1}, respectively, higher than their global minima, so they are less likely to be observed in the experiments. The structures and relative energies of isomers are given in Fig. S5–S7 (ESI†).

We further examined the kinetic stability of the global minima (**1**, **4**, and **6**), as well as the second lowest isomer **2** by performing 50 ps BOMD simulations at the B3LYP/BSII level and 298 K. The kinetic stability is evaluated by examining the structural evolution during the simulation, which is measured by the root-mean-square deviation (RMSD, relative to the B3LYP/BSII-optimized structures). As shown in Fig. 4, the RMSDs of **1**, **2**, and **4** (**A–C**) only fluctuate slightly around 0.5 Å, indicating their good kinetic stability. However, the RMSD values of **6** (**D**) gradually increase to large values (>2.5 Å), thus **6** is poor in terms of kinetic stability. Taken together, the stability studies

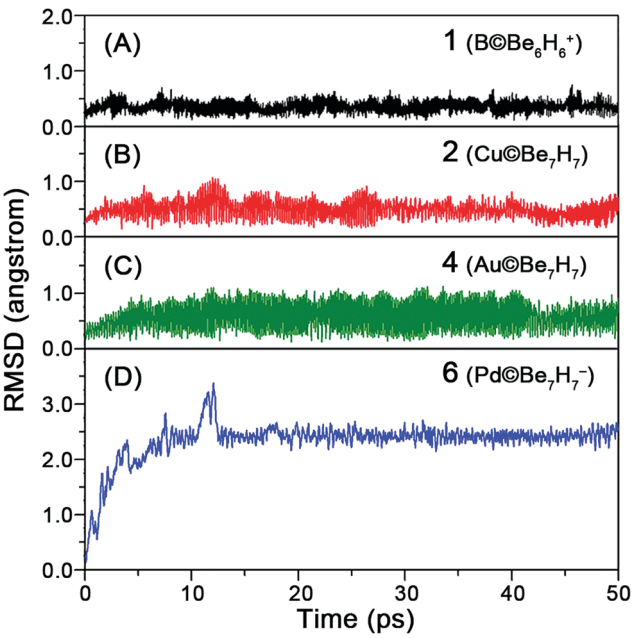

Fig. 4 RMSD *versus* simulation time for BOMD simulations of global energy minima **1**, **2**, **4**, and **6** at 298 K.

reveal that **1**, **2**, and **4** are kinetically stable global minima and could be promising targets for experimental preparations.

Conclusions

We have shown that Be_nH_n rings can act as *n*-electron σ-donors to accommodate an atom at center by complying with the octet or 18e rules, forming star-like $X©Be_nH_n$ species. Systematic screening on the combinations of Be_nH_n and X resulted in ten energy minima, among which $B©Be_6H_6^+$, $Cu©Be_7H_7$, and $Au©Be_7H_7$ were confirmed to be kinetically stable global minima, thereby providing the promising targets for experimental preparations. Analyses on their electronic structures indicate that these species are stabilized by the σ-donation and π-backdonation between Be_nH_n ring and central atom, the σ–π double aromacticity, and the favorable Coulomb attraction among the negatively charged X center, positively charged Be_n middle layer, and negatively charged H_n outer layer. We expect this computational study can spur experimental interest to enrich the much less developed beryllium structural chemistry.

Conflicts of interest

There are no conflicts to declare.

Acknowledgements

This project is supported by NSFC (Grant No. 21720102006, 21273140, 21373216, 21471092, 21573233, 21773240, U1510103), the Special Program for Applied Research on Supercomputation of the NSFC-Guangdong Joint Fund (the second phase) (Grant No. U1501501), the Program for the Outstanding Innovative Teams of Higher Learning Institutions of Shanxi Province, the SXNSF (Grant No. 2012021007-3), the STIP Program (Grant No. 2017170), and the high performance computing platform of Shanxi University.

References

1 (*a*) F. A. Cotton, G. Wilkinson, C. A. Murillo and M. Bochmann, *Advanced Inorganic Chemistry*, Wiley-Interscience, New York, 6th edn, 1999; (*b*) N. N. Greenwood and A. Earnshaw, *Chemistry of the Elements*, Elsevier Ltd, Leeds, 2nd edn, 1997.

2 (*a*) R. Hoffmann, R. W. Alder and C. F. Wilcox Jr, *J. Am. Chem. Soc.*, 1970, **92**, 4992; (*b*) R. Keese, *Chem. Rev.*, 2006, **106**, 4787; (*c*) L. M. Yang, E. Ganz, Z. F. Chen, Z. X. Wang and P. v. R. Schleyer, *Angew. Chem., Int. Ed.*, 2015, **54**, 9468; (*d*) K. Exner and P. v. R. Schleyer, *Science*, 2000, **290**, 1937; (*e*) Z. X. Wang and P. v. R. Schleyer, *Science*, 2001, **292**, 2465; (*f*) R. M. Minyaev, T. N. Gribanova, V. I. Minkin, A. G. Starikov and R. Hoffmann, *J. Org. Chem.*, 2005, **70**, 6693; (*g*) Y. Pei and X. C. Zeng, *J. Am. Chem. Soc.*, 2008, **130**, 2580; (*h*) X. J. Wu, Y. Pei and X. C. Zeng, *Nano Lett.*, 2009, **9**, 1577; (*i*) Z. H. Cui, M. Contreras, Y. H. Ding and G. Merino, *J. Am. Chem. Soc.*, 2011, **133**, 13228; (*j*) X. Y. Luo, J. H. Yang, H. Y. Liu, X. J. Wu, Y. C. Wang, Y. M. Ma, S. H. Wei, X. G. Gong and H. J. Xiang, *J. Am. Chem. Soc.*, 2011, **133**, 16285.

3 (*a*) L.-S. Wang, *Int. Rev. Phys. Chem.*, 2016, **35**, 69; (*b*) A. P. Sergeeva, I. A. Popov, Z. A. Piazza, W. L. Li, C. Romanescu, L. S. Wang and A. I. Boldyrev, *Acc. Chem. Res.*, 2014, **47**, 1349.

4 (*a*) R. Islas, T. Heine, K. Ito, P. v. R. Schleyer and G. Merino, *J. Am. Chem. Soc.*, 2007, **129**, 14767; (*b*) J. C. Guo, W. Z. Yao, Z. Li and S. D. Li, *Sci. China, Ser. B: Chem.*, 2009, **52**, 566; (*c*) Y. L. Liao, C. L. Cruz, P. v. R. Schleyer and Z. F. Chen, *Phys. Chem. Chem. Phys.*, 2012, **14**, 14898; (*d*) C. Romanescu, T. R. Galeev, W. L. Li, A. I. Boldyrev and L. S. Wang, *Acc. Chem. Res.*, 2013, **46**, 350.

5 (*a*) S. Erhardt, G. Frenking, Z. F. Chen and P. v. R. Schleyer, *Angew. Chem., Int. Ed.*, 2005, **44**, 1078; (*b*) Y. B. Wu, C. X. Yuan and P. Yang, *THEOCHEM*, 2006, **765**, 35; (*c*) Z.-H. Cui, W.-S. Yang, L. Zhao, Y.-H. Ding and G. Frenking, *Angew. Chem., Int. Ed.*, 2016, **55**, 7841; (*d*) J.-C. Guo, L. Y. Feng, Y.-J. Wang, S. Jalife, A. Vasquez-Espinal, J. L. Cabellos, S. Pan, G. Merino and H.-J. Zhai, *Angew. Chem., Int. Ed.*, 2017, **56**, 10174.

6 M. Yanez, P. Sanz, O. Mo, I. Alkorta and J. Elguero, *J. Chem. Theory Comput.*, 2009, **5**, 2763.

7 (*a*) O. Mo, M. Yanez, I. Alkorta and J. Elguero, *J. Chem. Theory Comput.*, 2012, **8**, 2293; (*b*) L. Albrecht, R. J. Boyd, O. Mo and M. Yanez, *Phys. Chem. Chem. Phys.*, 2012, **14**, 14540; (*c*) M. Yanez, O. Mo, I. Alkorta and J. Elguero, *Chem. Phys. Lett.*, 2013, **590**, 22; (*d*) O. Mo, M. Yanez, I. Alkorta and J. Elguero, *Mol. Phys.*, 2014, **112**, 592; (*e*) M. Liu, L. Yang, Q. Li, W. Li, J. Cheng, B. Xiao and X. Yu, *J. Mol. Model.*, 2016, **22**, 192; (*f*) D. Yu, D. Wu, Y. Li and S. Y. Li, *Theor. Chem. Acc.*, 2016, **135**, 112; (*g*) K. M. El, G. L. Bendazzoli, S. Evangelisti, W. Helal, T. Leininger, L. Tenti and C. Angeli, *J. Phys. Chem. A*, 2014, **118**, 6664; (*h*) W. Helal, S. Evangelisti, T. Leininger and A. Monari, *Chem. Phys. Lett.*, 2013, **568**, 49; (*i*) Q. N. Zhang, W. L. Li, L. L. Zhao, M. H. Chen, M. F. Zhou, J. Li and G. Frenking, *Chem. – Eur. J.*, 2017, **23**, 2035; (*j*) O. Brea, I. Alkorta, O. Mo, M. Yanez, J. Elguero and I. Corral, *Angew. Chem., Int. Ed.*, 2016, **55**, 8736; (*k*) A. V. Mitin, *Chem. Phys. Lett.*, 2017, **682**, 30; (*l*) A. Bauza and A. Frontera, *Chem. – Eur. J.*, 2017, **23**, 5375.

8 R. Puchta, *Nat. Chem.*, 2011, **3**, 416.

9 C. Yuan, X.-F. Zhao, Y.-B. Wu and X. Wang, *Angew. Chem., Int. Ed.*, 2016, **55**, 15651.

10 (*a*) Z. X. Wang, C. G. Zhang, Z. F. Chen and P. v. R. Schleyer, *Inorg. Chem.*, 2008, **47**, 1332; (*b*) Y. B. Wu, J. L. Jiang, R. W. Zhang and Z. X. Wang, *Chem. – Eur. J.*, 2010, **16**, 1271; (*c*) J. O. C. Jimenez-Halla, Y. B. Wu, Z. X. Wang, R. Islas, T. Heine and G. Merino, *Chem. Commun.*, 2010, **46**, 8776; (*d*) B. Xiao, Y. H. Ding and C. C. Sun, *Phys. Chem. Chem. Phys.*, 2011, **13**, 2732; (*e*) A. C. Castro, G. Martinez-Guajardo, T. Johnson, J. M. Ugalde, Y.-B. Wu, J. M. Mercero, T. Heine, K. J. Donald and G. Merino, *Phys. Chem. Chem. Phys.*, 2012, **14**, 14964; (*f*) Y. B. Wu, Y. Duan, H. G. Lu and S. D. Li, *J. Phys. Chem. A*, 2012, **116**, 3290; (*g*) Y.-B. Wu, Y. Duan, G. Lu, H.-G. Lu, P. Yang, P. v. R. Schleyer,

G. Merino, R. Islas and Z.-X. Wang, *Phys. Chem. Chem. Phys.*, 2012, **14**, 14760; (*h*) Y. F. Li, Y. L. Liao and Z. F. Chen, *Angew. Chem., Int. Ed.*, 2014, **53**, 7248; (*i*) R. Grande-Aztatzi, J. L. Cabellos, R. Islas, I. Infante, J. M. Mercero, A. Restrepo and G. Merino, *Phys. Chem. Chem. Phys.*, 2015, **17**, 4620; (*j*) J. C. Guo, G. M. Ren, C. Q. Miao, W. J. Tian, Y. B. Wu and X. T. Wang, *J. Phys. Chem. A*, 2015, **119**, 13101; (*k*) B. Xiao, J. B. Cheng, Z. B. Liu, Q. Z. Li, W. Z. Li, X. Yang and X. F. Yu, *RSC Adv.*, 2015, **5**, 73945; (*l*) Y. Wang, F. Li, Y. F. Li and Z. F. Chen, *Nat. Commun.*, 2016, **7**, 11488; (*m*) X. Wang, Q. Wang, C. Yuan, X. F. Zhao, J. J. Li, D. Li, Y. B. Wu and X. T. Wang, *Phys. Chem. Chem. Phys.*, 2016, **18**, 11942; (*n*) J.-J. Li, Y. Mu, X. Tian, C. Yuan, Y.-B. Wu, Q. Wang, D. Li, Z.-X. Wang and S.-D. Li, *J. Mater. Chem. C*, 2017, **5**, 408; (*o*) C.-S. Liu, H.-H. Zhu, X.-J. Ye and X.-H. Yan, *Nanoscale*, 2017, **9**, 5854; (*p*) X. F. Zhao, H. X. Li, C. X. Yuan, Y. Q. Li, Y. B. Wu and Z. X. Wang, *J. Comput. Chem.*, 2016, **37**, 261; (*q*) J. C. Guo, W. J. Tian, Y. J. Wang, X. F. Zhao, Y. B. Wu, H. J. Zhai and S. D. Li, *J. Chem. Phys.*, 2016, **144**, 244303.

11 (*a*) T. J. Tague and L. Andrews, *J. Am. Chem. Soc.*, 1993, **115**, 12111; (*b*) P. F. Bernath, A. Shayesteh, K. Tereszchuk and R. Colin, *Science*, 2002, **297**, 1323; (*c*) A. Shayesteh, K. Tereszchuk, P. F. Bernath and R. Colin, *J. Chem. Phys.*, 2003, **118**, 3622; (*d*) X. F. Wang and L. Andrews, *Inorg. Chem.*, 2005, **44**, 610; (*e*) A. Zaluska, L. Zaluski and J. O. Strom-Olsen, *J. Alloys Compd.*, 2000, **307**, 157; (*f*) S. Sampath, A. I. Kolesnikov, K. M. Lantzky and J. L. Yarger, *J. Chem. Phys.*, 2008, **128**, 134512; (*g*) E. Mamontov, A. I. Kolesnikov, S. Sampath and J. L. Yarger, *Sci. Rep.*, 2017, **7**, 16244.

12 A. E. Reed, L. A. Curtiss and F. Weinhold, *Chem. Rev.*, 1988, **88**, 899.

13 (*a*) P. v. R. Schleyer, C. Maerker, A. Dransfeld, H.-J. Jiao and N. J. R. E. Hommes, *J. Am. Chem. Soc.*, 1996, **118**, 6317; (*b*) P. v. R. Schleyer, H. Jiao, N. J. R. v. E. Hommes, V. G. Malkin and O. Malkina, *J. Am. Chem. Soc.*, 1997, **119**, 12669; (*c*) Z. F. Chen, C. S. Wannere, C. Corminboeuf, R. Puchta and P. v. R. Schleyer, *Chem. Rev.*, 2005, **105**, 3842.

14 (*a*) D. Y. Zubarev and A. I. Boldyrev, *Phys. Chem. Chem. Phys.*, 2008, **10**, 5207; (*b*) D. Y. Zubarev and A. I. Boldyrev, *J. Org. Chem.*, 2008, **73**, 9251.

15 M. Saunders, *J. Comput. Chem.*, 2004, **25**, 621.

16 (*a*) Y. C. Wang, J. A. Lv, L. Zhu and Y. M. Ma, *Phys. Rev. B: Condens. Matter Mater. Phys.*, 2010, **82**, 094116; (*b*) Y. C. Wang, J. Lv, L. Zhu and Y. M. Ma, *Comput. Phys. Commun.*, 2012, **183**, 2063.

17 (*a*) J. M. Millam, V. Bakken, W. Chen, W. L. Hase and H. B. Schlegel, *J. Chem. Phys.*, 1999, **111**, 3800; (*b*) X. S. Li, J. M. Millam and H. B. Schlegel, *J. Chem. Phys.*, 2000, **113**, 10062.

18 H. G. Lu and Y. B. Wu, *GXYZ 2.0*, Shanxi University, Taiyuan China, 2015.

19 The CALYPSO program can be downloaded at http://www.calypso.cn/.

20 H.-J. Werner, *et al.*, *MolPro 2012.1*, University College Cardiff Consultants Limited, Cardiff UK, 2012.

21 M. J. Frisch, *et al.*, *Gaussian 09 Revision D.01*, Gaussian Inc., Wallingford CT, 2013.

